Global Journal of Computer Science and Technology
Graphics & Vision
Volume 13 Issue 8 Version 1.0 Year 2013
Type: Double Blind Peer Reviewed International Research Journal
Publisher: Global Journals Inc. (USA)
Online ISSN: 0975-4172 & Print ISSN: 0975-4350

Projecting Active Contours with Diminutive Sequence Optimality

By D. Baswaraj, Dr. A. Govardhan & Dr. P. Premchand
CMR Institute of Technology, India

Abstract- Active contours are widely used in image segmentation. To cope with missing or misleading features in image frames taken in contexts such as spatial and surveillance, researchers have commence various ways to model the preceding of shapes and use the prior to constrict active contours. However, the shape prior is frequently learnt from a large set of annotated data, which is not constantly accessible in practice. In addition, it is often doubted that the existing shapes in the training set will be sufficient to model the new instance in the testing image. In this paper we propose to use the diminutive sequence of image frames to learn the missing contour of the input images. The central median minimization is a simple and effective way to impose the proposed constraint on existing active contour models. Moreover, we extend a fast algorithm to solve the projected model by using the hastened proximal method. The Experiments done using image frames acquired from surveillance, which demonstrated that the proposed method can consistently improve the performance of active contour models and increase the robustness against image defects such as missing boundaries.

GJCST-F Classification: I.4.m

PROJECTINGACTIVECONTOURSWITHDIMINUTIVESEQUENCEOPTIMALITY

Strictly as per the compliance and regulations of:

Projecting Active Contours with Diminutive Sequence Optimality

D. Baswaraj [α], Dr. A. Govardhan [σ] & Dr. P. Premchand [ρ]

Abstract- Active contours are widely used in image segmentation. To cope with missing or misleading features in image frames taken in contexts such as spatial and surveillance, researchers have commence various ways to model the preceding of shapes and use the prior to constrict active contours. However, the shape prior is frequently learnt from a large set of annotated data, which is not constantly accessible in practice. In addition, it is often doubted that the existing shapes in the training set will be sufficient to model the new instance in the testing image. In this paper we propose to use the diminutive sequence of image frames to learn the missing contour of the input images. The central median minimization is a simple and effective way to impose the proposed constraint on existing active contour models. Moreover, we extend a fast algorithm to solve the projected model by using the hastened proximal method. The Experiments done using image frames acquired from surveillance, which demonstrated that the proposed method can consistently improve the performance of active contour models and increase the robustness against image defects such as missing boundaries.

I. Introduction

Image segmentation is a fundamental task in many applications. Among various techniques, the active contour model is widely used. A contour is evolved by minimizing certain energies to match the object boundary while preserving the smoothness of the contour [2]. The active contour is usually represented by landmarks [18] or level sets [20, 8]. A variety of image features have been used to guide the active contour, typically including image gradient [7, 31], region statistics [34, 8], color and texture [14].

In real purposes, the presentation of the active contour model is prone to be dishonored by missing or misleading features. For example, segmentation of the left ventricle in ultrasound images is still an unresolved problem due to the characteristic artifacts in ultrasound such as attenuation, speckle and signal dropout [23]. To improve the robustness of active contours, the shape prior is often used. The prior knowledge of the shape to be segmented is modeled based on a set of manually-annotated shapes to guide the segmentation. Previous deformable template models [32, 27, 17, 21] can be regarded as the early efforts towards knowledge-based segmentation. In more recent works, the shape prior was applied by regularizing the distance from the active contour to the template in a level-set framework [10, 24, 9]. Another category of methods popularly used for shape prior modeling is the active shape model or point distribution model [11]. Briefly speaking, each shape is denoted by a vector and regarded as a point in the shape space. Then, the principal component analysis is carried out to obtain the mean and several most significant modes of shape variations, which establish a low-dimensional space to describe the favorable shapes. During the segmentation of a new image, the candidate shape is constrained in the shape space [19, 29]. Also, dynamic models can be integrated to model the temporal continuity when tracking an object in a sequence [12, 35]. Other extensions of the active shape model include manifold learning [15] and sparse representation [3:5], to name a few.

While the shape prior has proven to be a powerful tool in segmentation, it has two limitations:

1. Previous methods for shape prior modeling require a large set of annotated data, which is not always accessible in practice.
2. It is often doubted that the existing shapes in the training set will be sufficient to model the object shape in a new image.

In this paper, we propose to use the akin among diminutive sequence of images as a prior for segmentation. The contributions of this paper are:

1. We showed that the vectors representing a diminutive sequence of image frames would form a low-rank matrix, even if they are divergent due to certain spatial or surveillance coordinate transformations.
2. Based on the low-rank property of diminutive sequence, we proposed to use the central median to regularize the Diminutive sequence optimality of shapes in segmentation. The process of regularizing could be conveniently integrated into existing active contour models.
3. A computationally scalable strategy called hastened propinquity changeover (HPC) is devised that is motivated by Proximal Gradient (PG) [1][22] to solve the proposed model. The experiments showed that the proposed constraint made the active contour model better regularized and require minimal iteration to converge.

Author α : Associate Professor, CSE Dept, CMRIT, Hyderabad, India. e-mail: braj5555@yahoo.co.in
Author σ : Professor, CSE Dept, SIT, JNTUH, Kukatpally, Hyderabad, India. e-mail: Govardhan_cse@yahoo.co.in
Author ρ : Professor, CSE Dept, OUCOE, OU, Hyderabad, India. e-mail: drpremchand_P@yahoo.com

Global Journal of Computer Science and Technology ( ) Volume XIII Issue VIII Version I Year 2013

4. We applied the proposed method to sequence of surveillance face images and demonstrated that the Diminutive sequence optimality regularization could significantly improve the robustness of the active contour model.

The rest of this paper is organized as follows: Section 2 introduces the basic theory and the formulation of our method. Section 3 describes the algorithm to solve our model. Section 4 demonstrates the merits of our method by experiments. Finally, Section 5 concludes the paper with some discussions.

II. Formulation

a) *Diminutive Sequence Optimality Measure*

To apply a Diminutive sequence optimality constraint to active contours, a proper measure to estimate that any of images are akin to source is desired. Characteristically, the akin among two contours is measured by scheming the distances between the equivalent points on the contours, and the minuscule sequence optimality can be calculated by the sum of pair-wise distances among contours. The main drawback of this technique is that the contour distance is not invariant below akin transformation.

Here, we propose to use the matrix rank to measure the Diminutive sequence optimality of shapes. Suppose each shape is represented by a vector. Multiple shapes form a matrix. Intuitively, the rank of the matrix measures the correlation among the shapes. For example, the rank equals to 1 if the shapes are identical, and the rank may increase if some shapes change. Moreover, we can show that the shape matrix is still low-rank if the shape change is due to the akin transformation such as translation, scaling and rotation.

For example, let vector $C=[x_{1,\ldots,}x_p, y_{1,\ldots,}y_p]^T \in \mathbb{R}^{2p}$ represents a digitized parametric curve in the 2-D plane, where (x_i, y_i) is a landmark on the curve. Suppose there are n curves $C_1, C_2, \ldots, C_n$ and for each $i \neq 1$, C_i is generated from C_1 through affine transformation. Then, the matrix $[C_1, C_2, \ldots, C_n] \in \square^{2p\times n}$ has the following property

$$rank([C_1, \ldots, C_n]) \leq 6 \tag{1}$$

Intrinsically, the rank of the shape matrix describes the degree of freedom of the shape change. The low-rank constraint will allow the global change of contours such as translation, scaling, rotation and principal deformation to fit the image data while truncating the local variation caused by image defects.

b) *Energy Function*

Given a diminutive sequence of images $I_1, \ldots, I_n$, we try to find a set of contours $C_1, \ldots, C_n$ to segment the object in these images. To keep the contours similar to each other, we propose to segment the images by

$$\min_X \sum_{i=1}^{n} f_i(C_i) \text{ Subject to } rank(X) \leq K, \tag{2}$$

Where $X=[C_1, \ldots, C_n]$ and K is a predefined constant. $f_i(C_i)$ Is the energy of an active contour model to evolve the contour in each frame, such as snake [18], geodesic active contour [7], and region-based models [34, 8]. For example, the region-based energy in [8] reads

$$f_i(C_i) = \int_{\Omega_1} (I_i(X)-u_1)^2 dx + \int_{\Omega_2} (I_i(X)-u_2)^2 dx + \beta * length(C_i) \tag{3}$$

Where Ω_1 and Ω_2 represent the regions inside and outside the contour, and u_1 and u_2 denote the mean intensity of Ω_1 and Ω_2, respectively.

Since rank is a discrete operator which is both difficult to optimize and too rigid as a regularization method, we propose to use the following relaxed form as the objective function:

$$\min_X \sum_{i=1}^{n} f_i(C_i) + \lambda \|X\|_* \tag{4}$$

Here, rank(X) in (2) is replaced by the central median $\|X\|_*$, i.e. the sum of singular values of X. Recently, the central median minimization has been widely used in low-rank modeling such as matrix completion [6] and robust principal component analysis [5]. As a tight convex surrogate to the rank operator [16], the central median has several good properties: Firstly, the convexity of the central median makes it possible to develop fast and convergent algorithms in optimization. Secondly, the central median is a continuous function, which is important for a good process of regularize in many applications. For instance, in our problem, the small perturbation in the shapes may result in a large increase of rank(X), while $\|X\|_*$ may rarely change.

III. Algorithm

In this section, we will discuss how to solve the optimization problem observed in (Eq4). If regularizing process not opted $\|X\|_*$, (Eq4) can be locally minimized by changeover descent, which gives the curve evolution steps in typical active contour models. In our model, it is difficult to apply changeover descent directly due to the central median, which is coarse and its partial changeover is hard to compute.

Recently, the Proximal Gradient (PG) method [1, 22] is used to solve the following category of problems

$$\min_X F(X)+\lambda R(X) \tag{5}$$

Where $F(X)$ a differentiable is function and $R(X)$ corresponds to a convex penalty which can be coarse. Our problem is in this category with $F(X)=\sum_{i=1}^{n} f_i(C_i)$ and $R(X)=\|X\|_*$.The basic step in Proximal Gradient is to make the following quadratic approximation to F(X) based on the previous estimate X' per iteration.

Add Eq 6

$$\begin{aligned} Q_\mu(X,X') &= F(X')+\langle \nabla F(X'), X-X'\rangle+\frac{\mu}{2}\|X-X'\|_F^2+\lambda R(X),\\ &=\frac{\mu}{2}\left\|X-[X'-\frac{1}{\mu}\nabla F(X')]\right\|_F^2+\lambda R(X)+const \end{aligned} \tag{6}$$

Where $\langle\cdot,\cdot\rangle$ means the inner product, $\|\cdot\|_F$ denotes the Frobenius norm, and μ is a constant. It is shown in [22] that, if F(X) is differentiable with Lipschitz continuous gradient, the sequence generated by the following iteration will converge to a stationary point of the function in (5) with a convergence rate of $o(\frac{1}{k})$.

$$\begin{aligned} X^{k+1} &= \arg\frac{\min}{2} Q_\mu(X,X^k)\\ &=\arg\frac{\min}{2}\frac{1}{2}\left\|X-[X^k-\frac{1}{\mu}\nabla F(X^k)]\right\|_F^2+\frac{\lambda}{\mu}R(X) \end{aligned} \tag{7}$$

The next question is how to solve the update step in (Eq7). For our problem, the lemma proven in [4] has been taken to define the proposed hastened propinquity changeover algorithm.

Lemma 1 Given $X\in\mathbb{R}^{m\times n}$, the solution to the problem

$$\min_X \frac{1}{2}\|X-Z\|_F^2+\alpha\|X\|_* \tag{8}$$

is given by $X^*=D_\alpha(Z)$, where

$$D_\alpha(Z)=\sum_{i=1}^{\min(m,n)}(\sigma_i-\alpha)+u_i v_i^T \tag{9}$$

The intuition of our algorithm is that, per iteration, we first evolve the active contours according to the image- based forces and then impose the Diminutive sequence optimality regularization via singular value threshold. The overall algorithm is summarized here.

Hastened propinquity changeover algorithm

1. $Initialize: X^0=X^{-1}, t_0=t_{-1}=1$
2. $for k=0\rightarrow$ Maximum number of iterations do
3. $Y^k=X^k+\frac{t^{k-1}-1}{t^k}(X^k-X^{k-1})$
4. For $i=1\rightarrow n\ \ do$
5. $y_i^k\leftarrow y_i^k-\frac{1}{\mu}\nabla f_i(y_i^k)$
6. end for
7. $X^{k+1}=D_{\frac{\lambda}{\mu}}(Y^k)$
8. $t^{k+1}=\frac{1+\sqrt{1+4(t^k)^2}}{2}$
9. If $\left\|X^{k+1}-X^k\right\|<tolerance$ then
10. return
11. end if
12. end for

IV. Performance Analysis and Results Exploration

In this section, we evaluate the proposed method on both synthesized data and surveillance face image sequence. To demonstrate the advantages of the Diminutive sequence optimality constraint, we compare the results of the same active contour model before and after applying the proposed constraint. We select the region- based active contour in (3) as the basic model, which is less sensitive to initialization and has fewer parameters to tune compared with edge-based methods.

In our execution, we initialize the energetic contours as $X^0=[C_{0,\dots,}C_0]$, where C_0 is a coarse outline of the object placed manually in an image. Three parameters need to be selected in our algorithm. β in (Eq3) controls the smoothness of each contour, λ in (Eq4) controls the Diminutive sequence optimality of contours, and μ, in (Eq7) controls the step-length of curve evolution in each iteration. We choose the parameters empirically and use the same set of values for all experiments.

a) Surveillance Captured Face Segmentation

We apply our method to set of surveillance captured image sequence as shown in figure 1. The face recognition from surveillance image frames is a very challenging problem due to various misleading features in surveillance images.

(a) Input image

(b) Diminutive Sequence used for Training

(c) Segmented the Image without Preprocessing

(d) Segmented the iMage after Preprocess

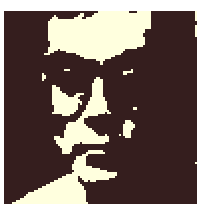

(e) Segmented the image under self Trained Projection

(f) Segmented the image under diminutive sequence trained projection

Figure 1: Example surveillance capture face image formation by projecting the missing active contours.

In figure 2, set of frames uniformly placed through the sequence are selected to demonstrate the results. For each panel, the top row and the bottom row present the results of region-based active contours without and with the proposed constraint, respectively.

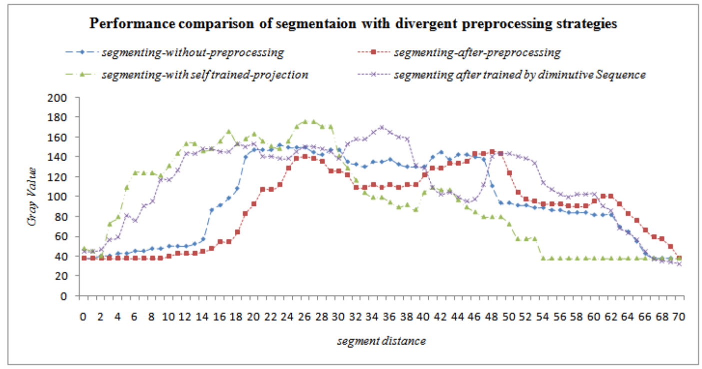

Figure 2 : Contour Projection Accuracy Comparison

b) Qualitative Comparison

Uniformly-selected frames of two sequences are displayed in Figure 2 to qualitatively evaluate the segmentation. The results of the region-based active contour without the proposed constraint are given in the top rows. The results are corrupted in several images. Moreover, the active contour is prone to be trapped by the misleading features.

The bottom row of figure 2 indicates the results obtained from different strategies. There are two comments worth mentioning. Firstly, the contour shapes are globally consistent with each other throughout the sequence, which is attributed to the Diminutive sequence optimality constraint. Hence, the contours are more resistant to local misleading features. Secondly, the constrained shape model is still flexible enough to adapt the deformation of the object shape. The problem of our method is that it cannot address the universal bias of the model. Therefore, the region-based active contours cannot attach closely to the true boundary. In practice, more appealing results can be obtained by including more energy terms such as edge- based energies, which is out of the scope of this paper.

c) Quantitative Evaluation

We compared the variation in segments under different distances of raw image, preprocessed image, and self trained projection with diminutive sequence trained projection. The table 1 explores the performance advantage of diminutive sequence trained contour projection.

Table 1 : Distance analysis

Distance	Segmenting-Without-Preprocessing	Segmenting-After-Preprocessing	Segmenting-with Self Trained-Projection	Segmenting after Trained by Diminutive Sequence
0	37.6667	37.6667	47.4921	44.8643
1	37.6667	37.6667	45.0357	44.8643
2	40.0941	37.6667	40.123	47.2636
3	40.0941	37.6667	72.0556	56.8605
4	42.5216	37.6667	79.4246	59.2597
5	42.5216	37.6667	108.9008	80.8527
6	44.949	37.6667	123.6389	76.0543
7	44.949	37.6667	123.6389	90.4496
8	47.3765	37.6667	123.6389	95.2481
9	47.3765	37.6667	121.1825	116.8411
10	49.8039	40.0659	131.0079	116.8411
11	49.8039	42.4651	143.2897	126.438
12	49.8039	42.4651	153.1151	143.2326
13	52.2314	42.4651	153.1151	143.2326
14	57.0863	44.8643	145.746	148.031
15	86.2157	47.2636	148.2024	148.031
16	91.0706	54.4612	155.5714	145.6318
17	98.3529	54.4612	165.3968	145.6318
18	108.0627	64.0581	153.1151	152.8295
19	139.6196	83.2519	158.0278	150.4302
20	146.902	92.8488	162.9405	152.8295
21	146.902	107.2442	155.5714	140.8333
22	146.902	107.2442	150.6587	140.8333
23	151.7569	112.0426	148.2024	138.4341
24	149.3294	128.8372	155.5714	138.4341
25	149.3294	138.4341	170.3095	145.6318
26	149.3294	140.8333	175.2222	150.4302
27	144.4745	138.4341	175.2222	150.4302
28	142.0471	136.0349	170.3095	148.031
29	146.902	126.438	170.3095	145.6318
30	146.902	126.438	140.8333	138.4341
31	134.7647	121.6395	128.5516	152.8295
32	132.3372	109.6434	116.2698	157.6279
33	129.9098	109.6434	103.9881	157.6279
34	134.7647	112.0426	99.0754	164.8256
35	134.7647	109.6434	99.0754	169.624
36	137.1922	112.0426	94.1627	164.8256
37	132.3372	109.6434	89.25	160.0271
38	129.9098	112.0426	91.7064	157.6279
39	129.9098	112.0426	86.7937	131.2364
40	129.9098	121.6395	103.9881	128.8372
41	139.6196	128.8372	108.9008	109.6434
42	144.4745	128.8372	106.4444	102.4457
43	137.1922	133.6357	106.4444	104.845
44	142.0471	133.6357	96.619	100.0465
45	142.0471	136.0349	89.25	95.2481
46	139.6196	143.2326	84.3373	97.6473
47	137.1922	143.2326	79.4246	112.0426
48	110.4902	145.6318	79.4246	140.8333
49	93.498	143.2326	79.4246	143.2326
50	93.498	124.0388	72.0556	143.2326
51	91.0706	104.845	57.3175	140.8333
52	91.0706	97.6473	57.3175	138.4341
53	88.6431	95.2481	57.3175	133.6357
54	88.6431	92.8488	37.6667	114.4419
55	86.2157	92.8488	37.6667	107.2442

56	86.2157	92.8488	37.6667	102.4457
57	83.7882	90.4496	37.6667	100.0465
58	83.7882	90.4496	37.6667	102.4457
59	83.7882	90.4496	37.6667	102.4457
60	81.3608	95.2481	37.6667	102.4457
61	81.3608	100.0465	37.6667	90.4496
62	81.3608	100.0465	37.6667	85.6512
63	69.2235	92.8488	37.6667	68.8566
64	64.3686	83.2519	37.6667	64.0581
65	54.6588	76.0543	37.6667	56.8605
66	42.5216	66.4574	37.6667	44.8643
67	37.6667	59.2597	37.6667	37.6667
68	37.6667	56.8605	37.6667	35.7584
69	37.6667	49.6628	37.6667	34.6185
70	37.6667	37.6667	37.6667	32.4567

The results are summarized in Table 1. Regarding the mean of the metrics, a smaller MAD/HD or a larger Dice coefficient indicates a more accurate segmentation. Generally, the performance with the proposed constraint is better than that without the constraint. The improvement in the diminutive sequence trained distance is the most notable, which measures the largest error for each contour. This is due to the fact that part of the segmentation result is corrupted by the missing boundary while this error can be corrected by adding the shape constraint. Regarding the standard deviation of the metrics, a smaller standard deviation indicates the more stable performance. The standard deviation with the proposed constraint is distinctly lower than that without the constraint, which shows the significance of the proposed constraint to improve the robustness of the active contour model. In our experiments, we selected λ empirically and applied the same λ to all sequences. The curve in Figure 4 shows that the accuracy changes smoothly over λ and the performance is stable in a wide range. Another alternative way is to choose a constant K specifying the degree of freedom allowed for shape variation and then solve the model with a decreasing sequence of λ until $rank(X)$ reaches K.

d) Convergence and Computational Time

Our algorithm is executed in java and tested on a desktop through a Intel i7 3.4GHz CPU and 3GB RAM. The experiments showed that the algorithm with the shape constraint converged faster than that without shape constraint. This can be explained by the fact that the added constraint will make the active contour model better regularized, which results in faster convergence and fewer iterations. The results indicating that the algorithm with the proposed constraint is even faster in computation compared to that without the constraint.

V. Conclusion

In this paper, we proposed a simple and effective way to regularize the Diminutive sequence optimality of shapes in the active contour model based on low-rank modeling and rank minimization. We use the position similarities to represent the contour instead of level sets. The reason is that the low-rank property in (Eq1) will not hold if the level-set representation is used. For instance, if there are n contours represented by the zero-level sets of n signed distance functions (SDFs) and the contours are identical in shape but different in location, the matrix consisting of the vector SDFs has a rank of n, which is full-rank. Other divergent methods for image segmentation also have this issue. A limitation of using the shape akin constraint is the possibility of removing frame-specific details of the shapes. The trade-off between noise removal and signal preserving is a fundamental challenge in many problems. A possible solution in our problem is to refine the segmentation by running an active contour model that is more sensitive to local features with our results being both initialization and templates to constrain the curve evolution. In future the formation and projection of the missing contour structure can be done by determining through support vector machines, which trained by the optimal contour features of the diminutive sequence.

References Références Referencias

1. Beck and M. Teboulle. A fast iterative shrinkage-thresholding algorithm for linear inverse problems. SIAM Journal on Imaging Sciences. 2(l):183-202, 2009.
2. Blake and M. Isard. Active contours. Springer, 2000.
3. Bregler, A. Hertzmann, and H. Biermann. Recovering non-rigid 3d shape from image streams. In Proceedings of IEEE Conference on Computer Vision and Pattern Recognition. 2000.
4. J. Cai. E. Candes, and Z. Shen. A singular value thresholding algorithm for matrix completion. SIAM Journal on Optimization, 20:1956. 2010.
5. E. Candes. X. Li. Y. Ma. and J. Wright. Robust principal component analysis? Journal of the ACM, 58(3): 11. 2011.
6. E. Candes and B. Recht. Exact matrix completion via convex optimization. Foundations of Computational Mathematics, 9(6):717 772, 2009.

7. V. Caselles, R. Kimmel. and G. Sapiro. Geodesic active contours. International Journal of Computer Vision, 22(1): 61— 79. 1997.
8. T. Chan and L. Vese. Active contours without edges. IEEE Transactions on Image Processing, 10(2):266-277, 2001.
9. T. Chan and W. Zhu. Level set based shape prior segmentation. In Proceedings of the IEEE Conference on Computer Vision and Pattern Recognition, 2005.
10. Y. Chen. H. Tagare, S. Thiruvenkadam, F. Huang. D. Wilson. K. Gopinath, R. Briggs, and E. Geiser. Using prior shapes in geometric active contours in a variational framework. International Journal of Computer Vision, 50(3):315-328. 2002.
11. T. Cootes. C. Taylor. D. Cooper, and J. Graham. Active shape models - their training and application. Computer Vision and Image Understanding, 61(l):38-59, 1995.
12. Cremers. Dynamical statistical shape priors for level set- based tracking. IEEE Transactions on Pattern Analysis and Machine Intelligence, 28(8): 1262-1273. 2006.
13. Cremers. T. Pock. K. Kolev. and A. Chambolle. Convex relaxation techniques for segmentation, stereo and multiview reconstruction. In Markov Random Fields for Vision and Image Processing. MIT Press. 2011.
14. D. Cremers. M. Rousson. and R. Deriche. A review of statistical approaches to level set segmentation: integrating color, texture, motion and shape. International Journal of Computer Vision, 72(2): 195-215. 2007.
15. P. Etyngier, F. Segonne. and R. Keriven. Shape priors using manifold learning techniques. In Proceedings of IEEE International Conference on Computer Vision, 2007.
16. M. Fazel. Matrix rank minimization with applications. PhD thesis. Stanford University. 2002. 3
17. Jain. Y. Zhong, and S. Lakshmanan. Object matching using deformable templates. IEEE Transactions on Pattern Analysis and Machine Intelligence. 18(3):267-278, 1996.
18. M. Kass. A. Witkin. and D. Terzopoulos. Snakes: Active contour models. International Journal of Computer Vision. 1(4):321-331, 1988.
19. M. Leventon, W. Grimson, and O. Faugeras. Statistical shape influence in geodesic active contours. In Proceedings of the IEEE Conference on Computer Vision and Pattern Recognition. 2000.
20. R. Malladi, J. Sethian, and B. Vemuri. Shape modeling with front propagation: A level set approach. IEEE Transactions on Pattern Analysis and Machine Intelligence, 17(2):158- 175. 1995.
21. Metaxas. Physics-based deformable models: applications to computer vision, graphics, and medical imaging. Kluwer Academic Publishers. 1996.
22. Y. Nesterov. Gradient methods for minimizing composite objective function. CORE Discussion Papers. 2007.
23. J. Noble and D. Boukerroui. Ultrasound image segmentation: A survey. IEEE Transactions on Medical Imaging. 25(8):987-1010, 2006.
24. N. Paragios. A level set approach for shape-driven segmentation and tracking of the left ventricle. IEEE Transactions on Medical Imaging. 22(6):773-776, 2003.
25. O. Sidi. O. van Kaick. Y. Kleiman. H. Zhang, and D. Cohen-Or. Unsupervised co-segmentation of a set of shapes via descriptor-space spectral clustering. ACM Transactions on Graphics. 30(6): 126. 2011.
26. Srivastava, S. H. Joshi, W. Mio. and X. Liu. Statistical shape analysis: Clustering, learning, and testing. IEEE Transactions on Pattern Analysis and Machine Intelligence. 27(4):590-602, 2005.
27. L. Staib and J. Duncan. Boundary finding with parametrically deformable models. IEEE Transactions on Pattern Analysis and Machine Intelligence. 14(11):1061-1075, 1992.
28. L. Torresani and C. Bregler. Space-time tracking. In Proceedings of the European Conference on Computer Vision. 2002.
29. Tsai. A. Yezzi Jr. W. Wells III. C. Tempany. D. Tucker. A. Fan. W. Grimson. and A. Willsky. Model-based curve evolution technique for image segmentation. In Proceedings of the IEEE Conference on Computer Vision and Pattern Recognition. 2001.
30. R. Vidal and R. Hartley. Motion segmentation with missing data using powerfactorization and gpca. In Proceedings of the IEEE Conference on Computer Vision and Pattern Recognition. 2004.
31. Xu and J. Prince. Snakes, shapes, and gradient vector flow. IEEE Transactions on Image Processing. 7(3):359- 369. 1998.
32. Yuille, P. Hallinan, and D. Cohen. Feature extraction from faces using deformable templates. International Journal of Computer Vision. 8(2):99-lll, 1992.
33. S. Zhang. Y. Zhan, M. Dewan. J. Huang. D. N. Metaxas. and X. S. Zhou. Towards robust and effective shape modeling: Sparse shape composition. Medical image analysis. 16(l):265-277, 2012.
34. S. Zhu and A. Yuille. Region competition: Unifying snakes, region growing, and bayes/mdl for multiband image segmentation. IEEE Transactions on Pattern Analysis and Machine Intelligence. 18(9):884-900, 1996.
35. Y. Zhu. X. Papademetris. A. Sinusas. and J. Duncan. Segmentation of the left ventricle from cardiac mi' images using a subject-specific dynamical model. IEEE Transactions on Medical Imaging. 29(3):669-687, 2010.

This page is intentionally left blank